Environmental Science & Technology

Article

pubs.acs.org/est

Time- and Oil-Dependent Transcriptomic and Physiological Responses to *Deepwater Horizon* Oil in Mahi-Mahi (*Coryphaena hippurus*) Embryos and Larvae

Elvis Genbo Xu,[†] Edward M. Mager,[‡] Martin Grosell,[‡] Christina Pasparakis,[‡] Lela S. Schlenker,[‡] John D. Stieglitz,[‡] Daniel Benetti,[‡] E.Starr Hazard,[§,∥] Sean M. Courtney,[§] Graciel Diamante,[†] Juliane Freitas,[†] Gary Hardiman,[§,⊥] and Daniel Schlenk*[,†]

[†]Department of Environmental Sciences, University of California, Riverside, California 92521, United States

[‡]Department of Marine Biology and Ecology, University of Miami, Miami, Florida 33149, United States

[§]Center for Genomics Medicine, Medical University of South Carolina, Charleston, South Carolina 29403, United States

[∥]Computational Biology Resource Center, Medical University of South Carolina, Charleston, South Carolina 29403, United States

[⊥]Departments of Medicine & Public Health Sciences, Medical University of South Carolina, Charleston, South Carolina 29403, United States

Supporting Information

ABSTRACT: The Deepwater Horizon (DWH) oil spill contaminated the spawning habitats for numerous commercially and ecologically important fishes. Exposure to the water accommodated fraction (WAF) of oil from the spill has been shown to cause cardiac toxicity during early developmental stages across fishes. To better understand the molecular events and explore new pathways responsible for toxicity, RNA sequencing was performed in conjunction with physiological and morphological assessments to analyze the time-course (24, 48, and 96 h post fertilization (hpf)) of transcriptional and developmental responses in embryos/larvae of mahi-mahi exposed to WAF of weathered (slick) and source DWH oils. Slick oil exposure induced more pronounced changes in gene expression over time than source oil exposure. Predominant transcriptomic responses included alteration of EIF2 signaling, steroid biosynthesis, ribosome biogenesis and activation of the cytochrome P450 pathway. At 96 hpf, slick oil exposure resulted in significant perturbations in eye development and peripheral nervous system, suggesting novel targets in addition to the heart may be involved in the developmental toxicity of *DHW* oil. Comparisons of changes of cardiac genes with phenotypic responses were consistent with reduced heart rate and increased pericardial edema in larvae exposed to slick oil but not source oil.

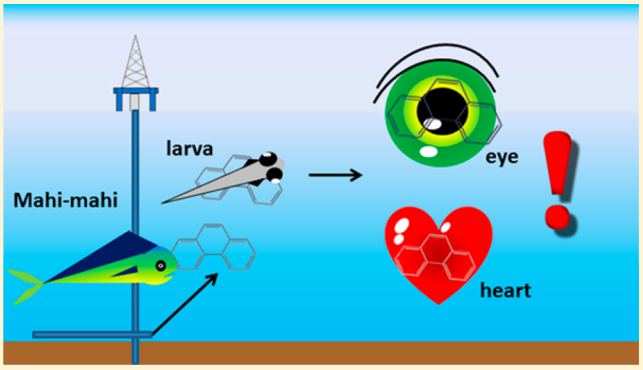

INTRODUCTION

The blow-out of the *Deepwater Horizon* (*DWH*) oil drilling platform initiated the largest oil release at depth in U.S. history, culminating in approximately three million barrels of crude oil released into the northern Gulf of Mexico over several months in the spring and summer of 2010.[1] The timing and location of oil release into the ecosystem from *DWH* coincided with the temporal spawning window for many economically and ecologically important pelagic fish species, such as mahi-mahi (*Coryphaena hippurus*) and yellowfin tuna (*Thunnus albacares*).[2,3] Crude oil-derived polycyclic aromatic hydrocarbons (PAHs) have been shown to adversely impact early life stage fish.[4,5] The composition and structure of individual PAHs in the water column can be significantly altered by natural weathering processes, and it has been shown that weathered surface slick oil is more toxic than source oil on a ∑PAH basis.[6] Weathering typically removes low molecular weight hydrocarbons from oil−water mixtures through evaporation, subsequently producing oil slicks with proportionally higher molecular weight and low solubility PAHs.[7]

The developing fish heart is a sensitive target organ for the toxic effects of crude oil-derived PAHs, particularly those containing three rings such as the phenathrenes, flourenes, and dibenzothiophenes.[5,8] The phenotypes of cardiotoxicity range from bradycardia, arrhythmias, contractility defects, atrium-to-ventricle conduction blockade, and eventually to heart failure.[9,10] In addition, oil exposed fish showed subtle changes

Received: May 3, 2016
Revised: June 23, 2016
Accepted: June 27, 2016
Published: June 27, 2016

DOI: 10.1021/acs.est.6b02205
Environ. Sci. Technol. 2016, 50, 7842−7851

in heart shape and reduction in swimming performance, indicative of reduced cardiac output.[4,11,12] The primary etiology of defects induced by PAHs has direct effects on cardiac conduction, which have secondary consequences for late stages of kidney development, neural tube structure, and formation of the craniofacial skeleton (eye and jaw).[13,14] Although the mutagenic and adverse whole-organismal effects of crude oil on fish development have been well recognized, the molecular initiating events are less understood. A recent study of select hypothesis-driven genes focusing on the developmental cardiotoxicity of crude oil exposure in mahi-mahi revealed a number of molecular indicators of cardiac stress and injury.[15] High throughput sequencing (HTS) allows unbiased quantification of expression levels of transcripts with a high sensitivity and broad genome coverage, and offers the potential to identify additional molecular indicators that are reflective of the PAH cardiotoxicity phenotype established by traditional microscopic analyses and may reveal other important, yet less overtly apparent, phenotypes and modes of action of oil exposure.

To help identify molecular mechanisms and pathways potentially involved in the developmental toxicity for fish exposed to *DWH* oil, transcriptomic profiles in mahi-mahi embryos exposed to different *DWH* oils (source and artificially weathered oil) were evaluated at different critical windows of development using HTS. Based on differentially expressed transcripts, the most impacted biological processes and pathways were identified at different developmental stages with multiple bioinformatic tools, providing novel insights into the mechanisms of *DWH* oil-induced developmental toxicities. The chemical composition and cardiotoxicity of different *DWH* oil types was also measured with the intent of anchoring the linkages between molecular, functional and morphometric end points during embryonic development.

MATERIALS AND METHODS

Animals. Mahi-mahi broodstock were captured off the coast of Miami, FL using hook and line angling techniques and subsequently transferred to the University of Miami Experimental Hatchery (UMEH) where they were acclimated in 80 m^3 fiberglass maturation tanks (typically 5−7 per tank). Tanks were equipped with recirculating aquaculture systems for water quality and temperature control. All embryos used in experiments were collected using standard UMEH methods.[16] A prophylactic formalin treatment (37 ppm formaldehyde solution for 1 h) was administered to the embryos, followed by a 0.5 h rinse with a minimum of 300% water volume using filtered, UV-sterilized seawater. Fertilization rate and embryo quality was assessed microscopically from a small sample of eggs collected from each spawn. Spawns with low fertilization rate (<85%) or frequent morphological abnormalities (>5%) were not used.

Preparation of Water Accommodated Fractions. Two sources of crude oil from the *DWH* spill that varied with respect to the state of weathering were obtained from British Petroleum under chain of custody for testing purposes: (1) slick oil collected from surface skimming operations (sample ID: OFS-20100719-Juniper-001 A0091G) and (2) oil from the Massachusetts barge (sample ID: SO-20100815-Mass-001 A0075K) which received oil collected from the subsea containment system positioned directly over the well (referred to herein as slick and source oil, respectively). Both types of oil were prepared as high energy water accommodated fractions (HEWAFs) on the day of use by mixing 1 g of oil per liter of 1 μm filtered, UV-sterilized seawater at low speed for 30 s in a Waring CB15 blender (Torrington, CT).[9] The mixture was immediately transferred to a glass separatory funnel, allowed to settle for 1 h and the lower ∼90% drained. The 100% HEWAF (unfiltered) was subsequently diluted in 1 μm filtered, UV-sterilized seawater to obtain test exposures.

Toxicity Testing. Three time course test solutions were subsequently performed using the nominal LC25s determined from the initial bioassays described in Supporting Information (SI) for the purposes of (1) RNA-Seq, (2) phenotypic anchoring of transcriptional responses by imaging analysis of heart rate and pericardial and yolk sac edema and (3) qPCR. The LC25 concentration was chosen as a compromise between attempting to capture initiating events as well as cascade effects while ensuring that a sufficient signal was observed. The first two exposures for RNA-Seq and imaging analysis were performed as described above with the following exceptions: three replicates were used per time point (24, 48, and 96 hpf) with 30 and 25 embryos/larvae per replicate, respectively. Animals hatch between 35 and 40 h. Slick and source oil HEWAF exposures were run concurrently using the same batch of embryos and a shared set of controls for both sets of experiments. The third time course exposure for qPCR was performed using only slick oil HEWAF in the same manner as the previous two exposures with five replicates and 25 embryos per replicate.

Image Analysis. Embryos or larvae were collected from each replicate beaker and imaged at 24, 48, and 96 h for assessment of heart rate and pericardial edema. Embryos or larvae were imaged using either a Fire-i400 or Fire-i530c digital camera (Unibrain, San Ramon, CA) mounted on a Nikon SMZ800 stereomicroscope. Images and videos were collected on a MacBook laptop using iMovie software and calibrated using a stage micrometer.

Water Chemistry Analysis. Samples for PAH analysis were collected in 250 mL amber bottles, stored at 4 °C and shipped overnight on ice to ALS Environmental (Kelso, WA) for analysis by gas chromatography/mass spectrometry−selective ion monitoring (GC/MS-SIM; based on EPA method 8270D). Initial (0 h) PAH samples were collected from bulk dilutions and final (24, 48, or 96 h) samples were composites of approximately equal volumes collected from each of the four corresponding replicates. Only initial samples were collected for control treatments. Reported ∑PAH values represent the sum of 50 select PAH analytes. Temperature, pH, dissolved oxygen (DO) and salinity were also measured (see SI). A summary of all measured water quality parameters and ∑PAH concentrations are provided in SI Tables S1−S3.

RNA Isolation, cDNA Library Construction and Sequencing. Three biological replicates were collected per treatment group. The surviving embryos or larvae from each replicate were pooled and homogenized with a Kontes Pellet Pestle Cordless Motor (Sigma-Aldrich, St. Louis, Missouri) in RNAzol (Molecular Research Center, Cincinnati, Ohio). RNA was isolated and purified with RNeasy Mini Kit (Qiagen, Valencia, CA). The total RNA sample was quantified by NanoDrop ND-1000 Spectrophotometer (Nanodrop Technologies, Wilmington, DE). RNA degradation and contamination were assessed on 1% agarose gels. RNA integrity was further verified using RNA 6000 Nano Assay chips run in Agilent 2100 Bioanalyzer (Agilent Technologies, Palo Alto, CA). 200 ng of total RNA was used to prepare RNA-Seq libraries using the TruSeq RNA Sample Prep kit following the protocol described

DOI: 10.1021/acs.est.6b02205
Environ. Sci. Technol. 2016, 50, 7842−7851

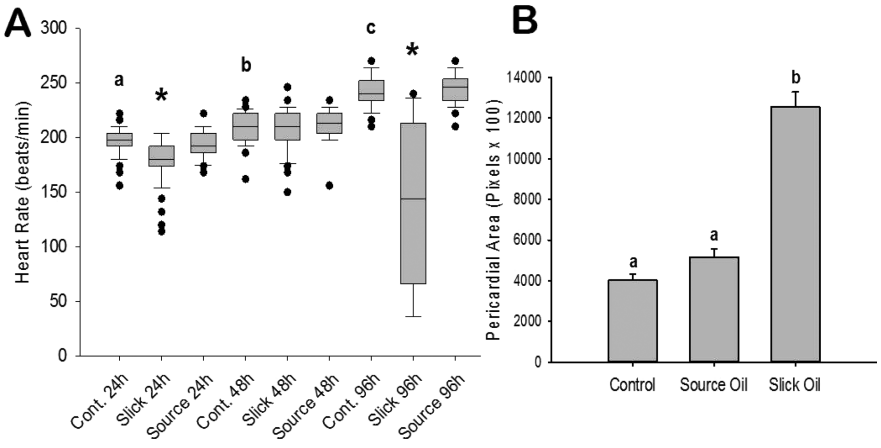

Figure 1. Time course of heart rate assessment in embryonic (24 h) and larval (48–96 h) mahi-mahi exposed to slick or source oil HEWAF (12 and 4.6 μg L^{-1} $\sum$PAHs, respectively) (A). Sample sizes are as follows (from left to right): 60, 57, 60, 42, 53, 48, 47, 25, and 46. Data are presented as box plots indicating the 25th and 75th percentiles; whiskers indicate the 90th and 10th percentiles; filled circles indicate outliers; solid and dashed lines indicate the median and mean, respectively. *Significantly different from time-matched control and source oil treatments by Kruskal–Wallis One Way Analysis of Variance on Ranks followed by Dunn's pairwise multiple comparison procedure. Letters indicate significant differences using the aforementioned statistical method. Pericardial area measured in yolk sac larvae at 48 h exposed to source and slick oil HEWAF (12 and 4.6 μg L^{-1} $\sum$PAHs, respectively) (B). Sample sizes are as follows (from left to right): 42, 52, and 47. Data are presented as mean ± SEM *Different letters* indicate significant differences in pericardial area between control and oil exposed larvae by Kruskal–Wallis One Way Analysis of Variance on Ranks followed by Dunn's pairwise multiple comparison procedure.

by the manufacturer (Illumina, San Diego, CA). Libraries were quantitated with NanoDrop, and four libraries were indexed and sequenced on one lane of an Illumina flow cell (TRUSEQ SBS V3). Single Read 1 × 50 sequencing was performed on an Illumina HiSeq 2500 at the Center for Genomics Medicine, Medical University of South Carolina, Charleston, SC, with each individual sample sequenced to a minimum depth of ~50 million reads (see SI Table S4 for details on sequencing QC and read depths).

Bioinformatic Analysis. Data were subjected to Illumina quality control (QC) procedures (>80% of the data yielded a Phred score of 30). Secondary analysis was carried out on an OnRamp Bioinformatics Genomics Research Platform (OnRamp Bioinformatics, San Diego, CA). OnRamp's advanced Genomics Analysis Engine utilized an automated RNaseq workflow to process the data, including (1) data validation and quality control, (2) read alignment to the *Takifugu rubripes* transcriptome (FUGU4) using BLASTX (against protein sequences): Basic Local Alignment Search Tool,[17] (3) generation of gene-level count data, and (4) differential expression analysis with DEseq2[18] (Genomics Research Platform with RNaseq workflow v1.0.1, including FastQValidator v0.1.1a, Fastqc v0.11.3, DESeq2:1.8.0). The resulting SAM files were sorted and run through the Python package HTSeq to generate count data for gene-level differential expression analyses. Transcript count data from DESeq2 analysis of the samples were sorted according to their adjusted *p*-value or *q*-value, which is the smallest false discovery rate (FDR) at which a transcript is called significant. FDR is the expected fraction of false positive tests among significant tests and was calculated using the Benjamini-Hochberg multiple testing adjustment procedure. The protein FASTA sequences from Ensembl for Fugu were compared using Ensembl's homology to create protein Fasta files that contained a human Entrez gene ID that mapped via *Fugu* to *Mahi-mahi*.

Statistical analysis of pathways and gene ontology (GO) terms was carried out using this sorted transcript list as described by us previously[19] and using Ingenuity Pathway Analysis (IPA, Qiagen, Valencia, CA), Advaita Pathway Guide,[20] and the ToppGene Suite.[21] The rationale behind using IPA, Advaita, and ToppGene is that the degree of annotation available for human is considerably greater than for fish species, and this permits a more sensitive systems level interrogation. Our methodology follows the premise that transcripts are sorted according to their q-value. As we have recently demonstrated releasing the FDR to 0.4 provides a larger gene list for downstream systems analyses. It should be noted that the GO and Pathway performed was itself subjected to FDR testing thereby adding statistical rigor to findings.[40,41]

Primer Design and Quantitative Reverse Transcription Real-Time PCR (qPCR). For targeted genes, National Center for Biotechnology Information (NCBI) nucleotide database was mined for available Perciform sequences (e.g., *Coryphaena hippurus, Notothenia coriiceps, Stegastes partitus, Oreochromis niloticus, Sciaenops ocellatus, Larimichthys crocea, Dicentrarchus labrax, Sparus aurata*, etc.) and available sequences were aligned with DNAMAN 8.0 (http://www.lynnon.com/). Identified regions of conservation were then targeted for qPCR primer design with PrimerQuest Tool (https://www.idtdna.com/Primerquest/Home/Index). Designed primers were target verified (≥80% sequence identity) by NCBI Primer-BLAST. Melt curve analysis and 1% agarose gel electrophoresis were performed to assess the specificity of the qPCR products. SI Table S5 shows the primers used in SYBR quantitative RT-PCR analysis. Differentially expressed genes identified by the above-described method were validated by qPCR using Power SYBR Green QPCR Master Mix (Life Technologies, Carlsbad, CA) on the iCycler-MyIQ (Bio-Rad, Hercules, CA) (see SI).

RESULTS

Chemical Composition of WAF. The PAH profiles exhibited by the slick oil and source oil HEWAFs differed markedly, reflecting the different degrees of weathering among the two oil types (see SI Figure S1, Table S6). The source oil was comprised predominantly of 2-ring PAHs (72%) followed

DOI: 10.1021/acs.est.6b02205
Environ. Sci. Technol. 2016, 50, 7842–7851

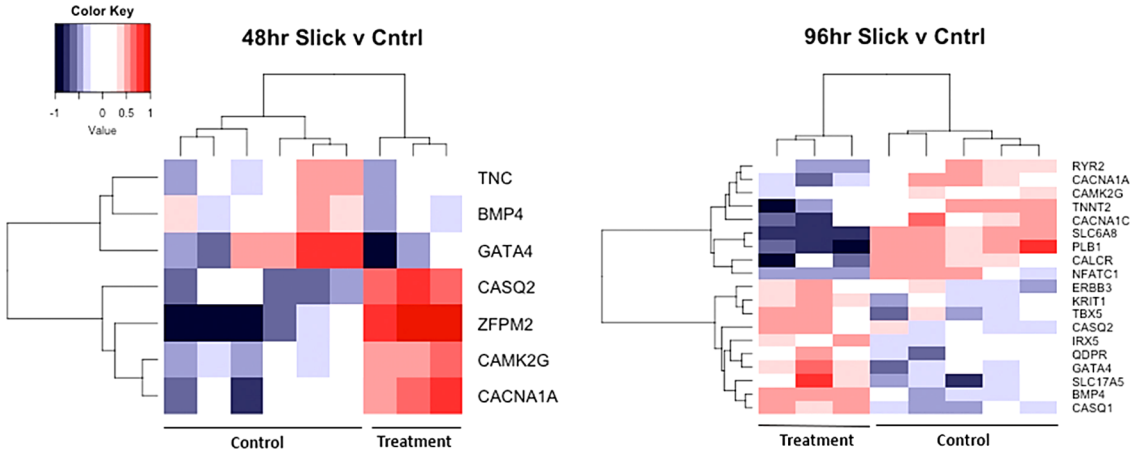

Figure 2. Heat map of gene expression changes in in 48 hpf (left) and 96 hpf (right) embryos in response to slick exposure. Red and blue boxes colors depict relative over- and under-expression in slick oil treated with respect to control. Samples and genes are clustered by similarity. The samples from each treatment group cluster together indicating gene expression differences for the represented transcripts between the two treatments.

by 3-ring PAHs (27%), represented largely by the napthalenes and phenanthrenes/anthracenes, respectively. By contrast, the slick oil was more weathered as evident by the loss of 2-ring PAHs (5%) and enrichment of 3-ring (69%) and 4-ring (25%) PAHs. Both profiles are similar to those obtained from HEWAF preparations using other sources of slick oil and source oil from the *DWH* spill.[6,11,15]

Toxicity Tests. Dose response regressions yielded 96 h % HEWAF LC25 values of 2.12 (0.80−3.09) and 0.09 (0.001−0.24) for the slick and source oils, respectively (values in parentheses indicate upper and lower 95% confidence intervals). Estimated 96 h ∑PAH LC50 values were calculated in two ways: using only the initial concentrations and the geometric mean of the initial and final concentrations. The estimated LC50s (in $\mu g\ L^{-1}$ ∑PAH) using both approaches were 19.5 (10.4−27.6) and 23.5 (12.9−31.25) for the slick oil and 16.5 (1.17−37.5) and 7.33 (0.72−17.5) for the source oil, respectively. The dose response curves for both 96 h bioassays using geometric mean ∑PAH concentrations are shown in SI Figure S2. Time courses of mean percent survival for the RNA-Seq, imaging and qPCR exposures are provided in SI Figure S3.

Physiological Measurements. The slick oil treatment significantly decreased heart rate at 24 and 96 h compared to both time-matched controls and source oil exposed fish (Figure 1A), and the effect was much more pronounced at 96 h. In addition, there was greater variability in heart rates observed among the slick oil treatment at all three time points with the greatest variability again at 96 h. It should be noted that many of the larvae in the 96 h slick oil treatment also exhibited highly variable heart rates (i.e., time interval between heartbeats). Finally, in control treatments heart rate was found to increase with age during this life stage. The slick oil treatment significantly increased pericardial area (see example in SI Figure S4) in larvae at 48 h compared to both controls and source oil exposed fish (Figure 1B).

Quality of Gene Expression Data. The unexposed control samples clustered separately from the slick or source oil treated sample, indicating global transcriptomic differences between the two sets (SI Figure S5).

Transcriptional Responses at 24 hpf after Slick and Source Oil Exposure. In 24 hpf embryos exposed to slick oil, 39 genes were significantly differentially expressed at a False Discovery Rate (FDR) < 0.1, and 95 genes were significantly differentially expressed at an FDR < 0.4 (SI Figure S6A). As for source oil exposure, 90 genes were significantly differentially expressed at FDR < 0.1, and 228 genes were significantly differentially expressed at FDR < 0.4. The significantly enriched Gene Ontology (GO) terms (molecular function, biological process) and Pathways were similar between slick and source oil exposure as assessed by ToppGene (SI Table S7). For the ontology of molecular function, 8 and 39 GO terms were significantly enriched after slick and source oil exposure, respectively. Structural constituents of ribosome and RNA binding were the predominant transcripts altered by oil exposure. Biological processes and pathways changed by oil exposure included transcripts involved in ribosome structure, translation termination, protein targeting to the endoplasmic reticulum, translational elongation, and cytoplasmic ribosomal proteins. IPA predicted an overall decreased activity in the Eukaryotic initiation factor 2 (EIF2) signaling pathway to cell viability in 24 hpf embryos by both slick and source oil exposure (SI Figure S7 A, B).

Transcriptional Responses at 48 hpf after Slick and Source Oil Exposure. Compared to 24 hpf, more genes were significantly altered at 48 hpf after slick and source oil exposure. The enriched GO terms were similar between 24 hpf and 48 hpf after source oil exposure. The most representative GO terms by source oil exposure included RNA binding, and were similar between time points with ribosome structure, translation termination, and protein targeting to the endoplasmic reticulum altered. However, significant differences between source and slick oil exposure started to occur at 48 hpf. In 48 hpf embryos after slick oil exposure, 196 genes were significantly differentially expressed at a FDR < 0.1, and 516 genes were significantly differentially expressed at a FDR < 0.4 (SI Figure S6B). ToppFun analysis using the ToppGene analysis suite revealed development and differentiation as the highest ranked biological functions, including cell development, tissue development, circulatory system development, cardiovascular system development, organ morphogenesis, neurogenesis, and cell morphogenesis (SI Table S8). Several genes (e.g., *casq2*, *cacna1a*) that were significantly differentially expressed after slick oil exposure are involved in cardiac muscle and Ca^{2+} homeostasis (Figure 2). The cardiovascular system

DOI: 10.1021/acs.est.6b02205
Environ. Sci. Technol. 2016, 50, 7842−7851

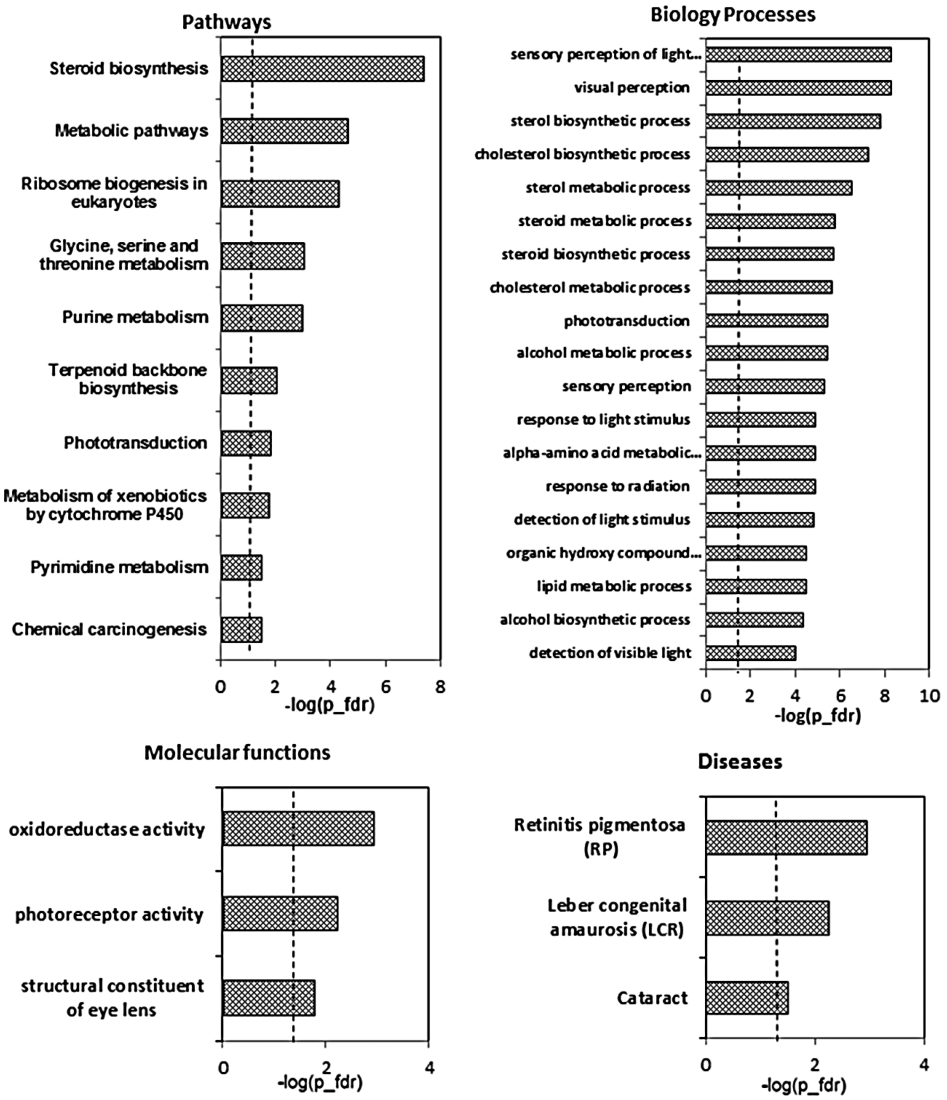

Figure 3. Predicted biological pathways and biological processes using the Advaita Pathway Guide. Mahi-mahi embryos were exposed to slick oil for 96 hpf. The *X*-axis is a negative log of the adjusted *p*-value.

phenotype was the first ranked enriched phenotype in 48 hpf by slick oil (SI Table S9). The significantly enriched canonical pathways included extracellular matrix organization, collagen biosynthesis, focal adhesion, metabolism, integrin signaling pathway, PI3K-Akt signaling pathway, pathways in cancer and metabolism of amino groups, and cardiomyopathy. The representative pathways are shown in SI Table S8. At the molecular level, the most represented GO terms were "binding", including sulfur compound binding, fibronectin binding, heparin binding, glycosaminoglycan binding, growth factor binding, cofactor binding, and collagen binding (SI Table S8). Enzyme binding (72 genes), transition metal ion binding (69 genes) and receptor binding (65 genes) were the top three molecular functions enriched in terms of the number of genes involved.

Transcriptional Responses at 96 hpf after Slick and Source Oil Exposure. The number of significantly differentially expressed genes (FDR < 0.1) greatly increased from 196 at 48 hpf to 1479 genes at 96 hpf after slick oil exposure (SI Figure S6). As for source oil exposure, 128 genes were significantly differentially expressed at FDR < 0.1, and 297 genes were significantly differentially expressed at FDR < 0.4. As with embryos at 24 and 48 hpf, *cyp1a1* was consistently the most strongly upregulated gene (26.5 fold) at 96 hpf after slick oil exposure. Similar to 48 hpf, the most significantly enriched GO molecular functions indicated by ToppGene in 96 hpf after source oil exposure were structural constituents of ribosomes, RNA binding, structural molecule activity, and oxidoreductase activity (SI Table S10). RNA binding was also the most significantly enriched molecular function in 96 hpf after slick oil exposure (>300 genes form input). According to biological function, there were some overlapping GO terms between slick and source oil exposures, such as cellular component disassembly, organic acid metabolic processes, and oxoacid metabolic processes, with many more genes altered after slick oil exposure than source oil exposure (SI Table S10). Extracellular matrix organization was the top enriched pathway in 96 hpf after source oil exposure. Metabolism and biosynthesis was the top enriched pathways identified by ToppFun in 96 hpf after slick oil exposure, including metabolism of amino acids and steroid biosynthesis (specifically cholesterol biosynthetic pathways). Comparing ToppFun and Advaita Pathway Guide analyses, both approaches were consistent with regard to the enriched GO pathways uncovered,

DOI: 10.1021/acs.est.6b02205
Environ. Sci. Technol. 2016, 50, 7842−7851

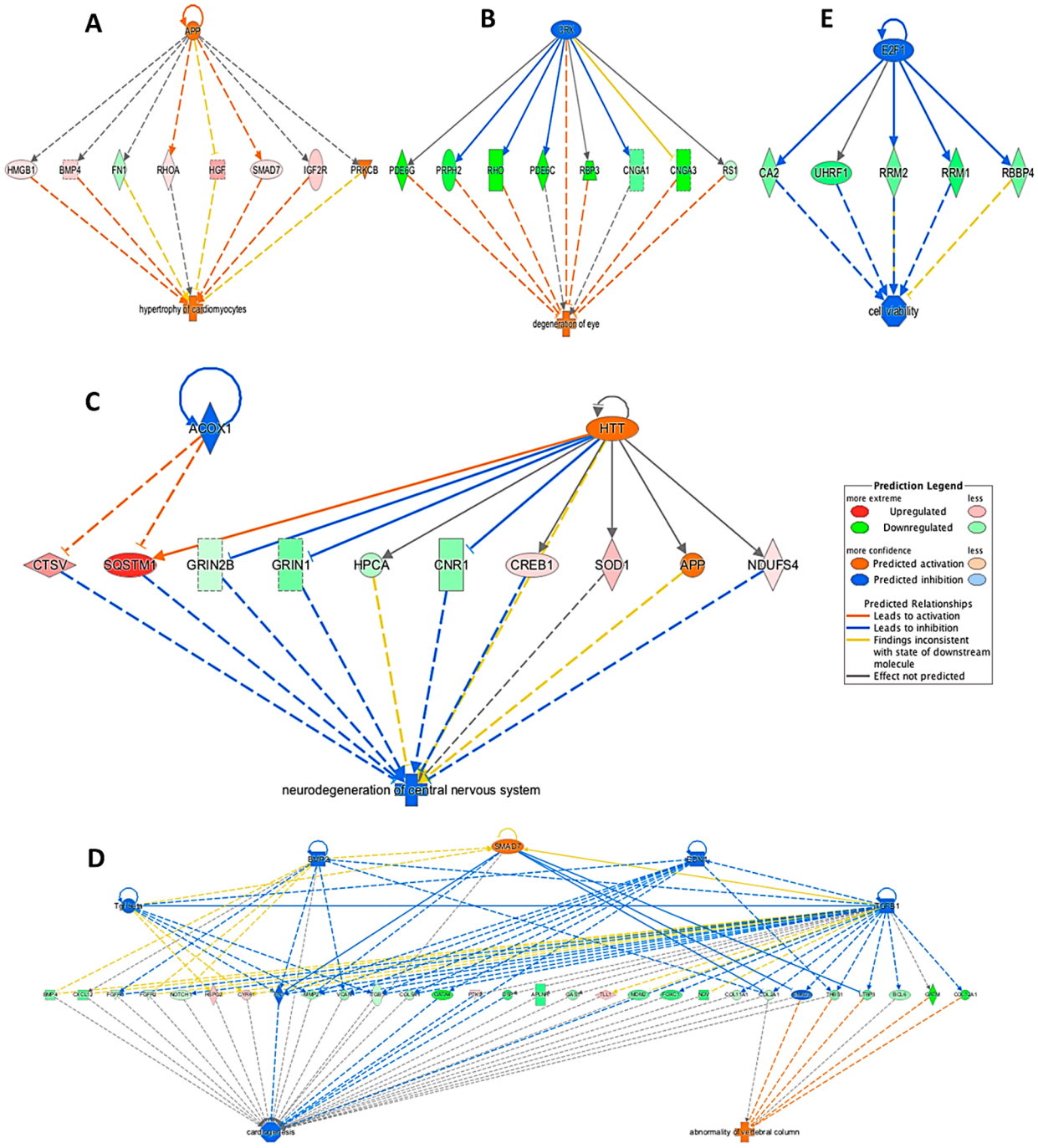

Figure 4. Predicted mechanisms through Ingenuity Pathway Analysis showing how WAF may lead to (A) hypertrophy of cardiomyocytes; (B) degeneration of the eyes; (C) neurodegeneration of central nervous system; (D) cardiogenesis and abnormal vertebral column; (E) decreased cell viability.

with steroid biosynthesis and metabolic pathways being the highest ranked pathways (Figure 3). Advaita also predicted that other biological processes, and molecular functions were altered, including visual perception, sterol biosynthetic processes, lipid metabolic processes, oxidoreductase activity, photoreceptor activity, as well as the disease pathways, retinitis pigmentosa, leber congenital amaurosis and cataract. Notably, 96 hpf after slick oil exposure, the genes involved in steroid biosynthesis were all significantly upregulated (SI Figure S8), while the genes involved in ribosome biosynthesis were all downregulated (SI Figure S9). At 96 hpf after slick oil exposure, ToppFun also identified abnormal cardiovascular system morphology as one of the phenotypes in 96 hpf after slick oil exposure (SI Table S11). Several genes differentially expressed after slick oil exposure were involved in cardiac muscle and Ca^{2+} homeostasis (Figure 2). IPA analysis further predicted the activation of hypertrophy of cardiomyocytes, and inhibition of cardiogenesis by slick oil exposure (Rank #5 Tox Functions predicted by IPA, Figure 4A). In comparison with slick oil, the transcriptomic profile in mahi-mahi embryos and larvae after source exposure were not significantly reflective of effects on cardiac muscle or Ca^{2+} homeostasis. In contrast to 24 hpf, IPA predicted an overall increased activity in EIF2 pathway at 96 hpf by both source and slick oil exposure (SI Figure S7 C, D).

DOI: 10.1021/acs.est.6b02205
Environ. Sci. Technol. 2016, 50, 7842−7851

Given the significant induction of *cyp1a1* in all time points receiving slick oil, IPA was also used to focus on aryl hydrocarbon receptor (AhR) pathways. Notably, 127 AhR-responsive genes were differentially expressed at 96 hpf larvae exposed to slick oil. The interaction between slick oil exposure and AhR largely upregulated the expression of *cyp1a1*, *cyp1b1*, *ugt1a1*, and *ahrr* at 96 hpf.

Validation of Differentially Expressed Genes by qRT-PCR. A subset of genes that were significantly up/down regulated in 96 hpf mahi-mahi larvae after oil exposure by RNaseq were quantified by qRT-PCR. Based on the HTS data, genes involved in the most significantly enriched GO terms or targeted organs by slick oil were selected (SI Figure S11). The genes include *rho* and *rgr* involved in eye development and phototransduction pathways (first ranked Biological Process in Figure 3; *p*-value = 4.8×10^{-9}); *sqle* in steroid biosynthesis (first ranked Pathway in Figure 3; p-value = 4.0×10^{-8}); *cyp1a1 and its upstream ahr, ahrr* in oxidoreductase activity (first ranked Molecular Function in Figure 3; *p*-value = 0.001); and *bmp4*, *gata4*, *cacna1a* involved in abnormal cardiovascular system morphology (Rank #16 Phenotype in SI Table S11; *p*-value $=7.5\times 10^{-4}$). Directions of change by RNaseq and qPCR were consistent with similar magnitudes of fold-change (SI Figure S11).

DISCUSSION

Many studies of fish embryo/larvae have indicated that PAHs associated with oil have caused cardiac phenotypes presenting pericardial edema.[4−10,13,14] While the Aryl hydrocarbon receptor (AhR) plays a role in the cardiotoxic phenotype particularly with tricyclic PAHs, the molecular connections between AhR activation and cardiotoxicity of oil is still unclear, particularly considering similar toxicities from other PAHs and oxygenated derivatives that are poor AhR ligands.[26] More recent studies have evaluated calcium and potassium homeostasis/function and indicate other molecular mechanisms may also be involved in the cardiac phenotype associated with oil toxicity in embryonic/larval stages in fish.[15,24,25] In the current study with mahi-mahi, several genes not associated with AhR were differentially expressed at 48 and 96 hpf after slick oil exposure and are involved in cardiac muscle and Ca^{2+} homeostasis (Figure 2). Proteins coded by *casq1* and *casq2*, calsequestrins, play important roles in maintaining the cellular Ca^{2+} levels and contraction of cardiac muscle. Cardiac ryanodine receptor 2 (*ryr2*) was significantly downregulated 96 hpf after slick oil exposure, also suggesting potential changes in cytosolic Ca^{2+} levels. Significant downregulation of troponin T type 2 (*tnnt2*) which regulates cardiac muscle contraction in response to alterations in intracellular calcium ion concentration[22] was observed in 96 hpf mahi-mahi larvae after slick oil exposure. Changes in this gene have been associated with cardiomyopathies in humans and chicken embryos.[23] *Camk2g* and *cacna1a* were significantly downregulated at 48 hpf but upregulated at 96 hpf (Figure 2). The product of camk2g belongs to the $Ca^{(2+)}$/calmodulin-dependent protein kinase subfamily, which is crucial for plasticity at glutamatergic synapses. Brette et al.[24] showed decreased calcium current (I_{Ca}) and calcium cycling, which disrupted excitation-contraction coupling in cardiomyocytes of bluefin tuna after slick oil exposure. We also found both L type and P/Q type voltage-dependent calcium channel genes were significantly downregulated in 96 hpf after slick oil exposure. It is possible that the decreased calcium channel expression and I_{Ca} levels may affect the cardiotoxicity of slick oil in mahi-mahi larvae. Besides cardiac and Ca^{2+} related pathways, some other organs and pathways were also identified as potential targets for slick oil.

To phenotypically link the affected cardiac associated genes to the higher order cardiac syndrome characteristic of crude oil exposure in fish, embryos and larvae were examined microscopically for a functional effect on heart rate (i.e., bradycardia) as well as pericardial and yolk sac edema. Slick oil exposure caused mild bradycardia at 24 hpf and 96 hpf, but not at 48 hpf, although pericardial edema was clearly increased at this time point. These findings are consistent with previous studies indicating that pericardial edema is the primary response and the most robust indicator of cardiac injury in mahi-mahi.[6,11,15] By contrast, source oil exposure did not induce bradycardia at any time point or cause cardiac edema, consistent with the lack of induced cardiac transcriptional responses to source oil exposure. It should be noted that although ∑PAH concentrations and composition were consistent across experiments for the respective oil types, notably higher mortality than the expected 25% was observed at 96 h for the slick oil imaging and qPCR experiments (57% and 50%, respectively; SI Figure S3). Still, responses at the molecular level were remarkably consistent when comparing genes analyzed by RNA-seq and qPCR (SI Figure S11) supporting a direct link between effects observed among the different experiments. Differences in PAH concentration/composition and acute mortality hinder direct comparisons among the slick and source oil exposures; nevertheless, the lack of functional or transcriptional cardiac effects by the latter likely reflects the lower ∑PAH concentrations and far lower relative abundance of the tricyclic PAHs for which the cardiotoxic phenotype is largely attributable.[8,13]

In addition to genes that indicated cardiac functional impairment, visual perception was the most significantly enriched process uniquely associated with the 96 hpf larvae after slick oil exposure (Figure 3), with 35 out of 70 differentially expressed genes identified in this biological pathway. Genes were associated with the series of events required for an organism to receive a visual stimulus, convert it to a molecular signal, and recognize and characterize the signal. In zebrafish embryos treated with the oxygenated PAH, 1,9-benz-10-anthrone, mRNAs associated with visual perception were also altered.[26] Advaita predicted that phototransduction was significantly suppressed by slick oil at 96 hpf. Consistent with this prediction, the transcript for rhodopsin (rho) was downregulated. *Rho* is an essential G-protein receptor, that when photoexcited, initiates the visual transduction cascade. Transducin (*gnat2*), and GMP-phosphodiesterase (*pde6g*) were also significantly downregulated. These two proteins play critical roles in stimulating the coupling of rhodopsin and cGMP, resulting in the closure of cGMP-gated cation channels subsequently leading to membrane hyperpolarization and release of neurotransmitters.[27] Recovery from light involves the deactivation of the photolyzed rhodopsin by rhodopsin kinase (encoded by *grk7* or *pk*, SI Figure S10); GTP-binding transducin alpha subunit is deactivated through a process that is stimulated by *rgs9* (SI Figure S10). Both *grk7* and *rgs9* were significantly downregulated, which could lead to the perturbation of rhodopsin regeneration and further phototransduction in the 96 hpf larvae by slick oil.

The top associated diseases included retinitis pigmentosa, leber congenital amaurosis and cataract formation (Figure 3). Slick oil may inhibit the activities of photoreceptor-specific

DOI: 10.1021/acs.est.6b02205
Environ. Sci. Technol. 2016, 50, 7842−7851

transcription factor *crx* and lead to downregulation of eye-associated gene expression and degeneration of eyes[28] (Figure 4B). Similarly, Huang et al.[14] used expression microarrays to predict ocular developmental toxicity by Benzo(a)pyrene (BaP), and linked the perturbation of photoreceptor related genes to a decreasing phototactic response behavior. In pufferfish larvae, oil exposure induced significantly smaller and shape-distorted eyes, and subsequent disrupted rhythmic motor movement, and suppressed positive phototaxis of larvae.[29] The authors suggested that the behavioral problems (incorrect swimming) could have originated from the abnormal visual sensation. The observed behavior problem would be significant, as it may cause severe disadvantages during fish life cycles by affecting feeding, escape, and migration responses.

Predictions by IPA also included the neurodegeneration of central nervous system and abnormality of the vertebral column in 96 hpf larvae after slick oil exposure (Figure 4C, D). We found four neurotransmitter transporter genes, *slc6A8* (creatine transporter), *slc6A18* (neutral amino acid transporter), *slc6A4* (serotonin transporter), and *slc6A2* (norepinephrine transporter) that were all significantly downregulated in 96 hpf larvae after slick oil exposure. Prenatal exposure to PAHs has been shown to induce neurological abnormalities such as cognitive impairment, learning difficulties, and loss of short-term memory.[30] Dibenzothiophene and phenanthrene disrupted neural tube structure, and pyrene induced neuronal cell death in zebrafish embryos.[13] BaP decreased brain mass, locomotor activity, dopaminergic neurons and resulted in neurodegeneration in zebrafish.[31] Although the mechanism of neurodegenerative diseases remains unclear, some genes are suggested to be associated with the occurrence of neurodegenerative diseases. A previous study demonstrated that SLC6A3 (solute carrier family 6 (neurotransmitter transporter), member 3) was significantly decreased in Parkinson's disease patients.[32] Gao et al.[31] also reported significantly downregulated SLC6A3 gene expression in zebrafish after BaP exposure.

Four *N*-methyl-D-aspartate receptor (NMDAR) genes (i.e., grin1, grin2a, grin2d and grin2b), and four Ca^{2+}/ calmodulin dependent kinase (CaMK) genes (i.e., *camk2a*, *camk2b*, *camk1g* and *camk2g*) were all significantly downregulated. Glutamate, a major excitatory neurotransmitter, stimulates the NMDAR, located primarily at synapses, causing a transient influx of Ca^{2+} into the postsynaptic neuron. Intracellular Ca^{2+}, along with calmodulin (CaM), can activate CaMKII.[33] As noted above with the cardiac impacts associated with altered Ca^{2+} metabolism, impairment affects many important neuronal processes, particularly in synaptic plasticity and memory.[34] The decrease of CaM and CaMK2 mRNA expression might contribute to altered synaptic plasticity and neuronal survival in exposure to benzo(a)pyrene-exposed rockfish embryos.[35] The downregulation of NMDAR and CaMK suggests neural toxicity may also be an additional target of slick oil through changes in glutamate receptor and Ca^{2+} homeostasis. Since Ca^{2+} appears to also play a significant role in cardiac toxicity, impairment in multiple targets may be responsible for a number of phenotypic responses besides that of cardiac toxicity that may adversely affect development at later life stages.

Another top ranked canonical pathway was the eukaryotic initiation factor 2 (EIF2) in both slick and source oil exposed mahi-mahi larvae at 24 and 96hpf by IPA. An overall decreased activity in the EIF2 signaling pathway at 24 hpf, but an increased activity at 96 hpf by both source and slick oil exposure was predicted. EIF2 plays a key role in global translation initiation and protein synthesis. The regulatory function of EIF2 is mediated via phosphorylation-dephosphorylation of its subunit α. Cellular stress can cause immediate phosphorylation of EIF2 subunit α, which results in inhibition of intracellular translation initiation as an adaptive response.[36] Phosphorylation at Ser 51 abrogates the function of EIF2 α and leads to a shutdown of global mRNA translation and consequently mobilizes stress induced gene expression involved in cell growth, differentiation and apoptosis.[37] EIF2 signaling was identified in the top 3 most significantly affected canonical pathways from the differential exon usage (DEU) genes in 96 hpf zebrafish larvae exposed to BaP.[38] Wang et al.[39] demonstrated that a benzo[a]pyrene metabolite BPDE induced severe cell cycle arrest, apoptosis and decreased cell viability in human amnion epithelial cells, and EIF2 α phosphorylation produced a pro-survival and antiapoptotic effect to alleviate the cellular damage. In the present study, the decreased activity in the EIF2 signaling pathway at 24 hpf followed by increased activity at 96 hpf by both source and slick oil exposure may indicate the 24 hpf stage is more susceptible to embryo lethality since the adaptive response was diminished. The relationship between the temporal responses (i.e., induction at 24 hpf and downregulation at 96 hpf) requires additional study to determine the role of this pathway in acclimation to PAH exposure.

Overall, this is the first study to investigate the time-course transcriptomic responses in marine fish embryos/larvae exposed to two types of *DWH* oil. Slick and source oil exposure induced similar transcriptional responses at early developmental stages (24 hpf), but transcript profiles were different at later developmental stages (48, 96 hpf) in mahi-mahi. IPA indicated slick oil exposure altered the EIF2 signaling which predicted loss of cell viability at early development stage, and induced differentially expressed cardiac-associated genes at 48 and 96 hpf. However, at 96 hpf, slick oil exposure resulted in pronounced perturbations in metabolism, steroid biosynthesis, visual, and cytochrome P450 genes suggesting other targets besides AhR pathways or the heart may be involved in the developmental toxicity of *DWH* oil. Using rapid genomics annotation analyses coupled with advanced informatics tools for a poorly annotated species that was impacted at the site of the *DWH* spill indicates these methods may be used in other species of concern to identify molecular and physiological responses of environmental contamination to reduce uncertainty in assessments of ecological risk and recovery of biota.

■ ASSOCIATED CONTENT

Supporting Information

The Supporting Information is available free of charge on the ACS Publications website at DOI: 10.1021/acs.est.6b02205.

Further information is available that provides PAH measurements (Figure S1; Table S6), water quality measurements (Table S1−S3), an example of larval pericardial edema (Figure S4), a heatmap showing the Euclidean distances between the samples (Figure S5), plots showing relative expression of genes (Figure S6), trends in EIF2 signaling (Figure S7), plots showing perturbations in steroid biosynthesis (Figure S8), ribosome biosynthesis (Figure S9) and phototransduction (Figure S10), primers used in qPCR (Table S5), the top predicted molecular functions, biological processes,

DOI: 10.1021/acs.est.6b02205
Environ. Sci. Technol. 2016, 50, 7842−7851

pathways and phenotype (Table S7−11), the full gene names in Figure 4 (Table S12), methods for determining $LC25_S$, water chemistry, pericardial area, transcript expression, and the standard Illumina QC procedures for mRNA sequencing data (Figure S12) (PDF)

AUTHOR INFORMATION

Corresponding Author

*Phone: 1-951-827-2018; e-mail: daniel.schlenk@ucr.edu.

Notes

The authors declare no competing financial interest.

ACKNOWLEDGMENTS

This research was made possible by a grant from The Gulf of Mexico Research Initiative. Grant No: SA-1520; Name: Relationship of Effects of Cardiac Outcomes in fish for Validation of Ecological Risk (RECOVER) M. Grosell holds a Maytag Chair of Ichthyology. GRIIDC DOI:10.7266/N7BG2M0. J. G. Hardiman acknowledges Medical University of South Carolina College of Medicine start-up funds. This research was supported in part by the Genomics Shared Resource, Hollings Cancer Center.

REFERENCES

(1) United States of America v. BP Exploration & Production, Inc., et al. 2015. Findings of fact and conclusions of law: Phase Two trial. In re: *Oil spill by the oil rig "Deepwater Horizon" in the Gulf of Mexico*, on April 20, 2010, No. MDL 2179, 2015 WL 225421 (LA. E.D. Jan. 15, 2015). (Doc. 14021). U.S. District Court for the Eastern District of Louisiana.

(2) Gibbs, R. H.; Collette, B. B. On the identification, distribution, and biology of the dolphins, *Coryphaena hippurus* and *C. equiselis*. *Bull. Mar. Sci.* **1959**, *9* (2), 117−152.

(3) Rooker, J. R.; Simms, J. R.; Wells, R. D.; Holt, S. A.; Holt, G. J.; Graves, J. E.; Furey, N. B. Distribution and habitat associations of billfish and swordfish larvae across mesoscale features in the gulf of Mexico. *PLoS One* **2012**, *7* (4), e34180.

(4) Hicken, C. E.; Linbo, T. L.; Baldwin, D. H.; Willis, M. L.; Myers, M. S.; Holland, L.; Larsen, M.; Stekoll, M. S.; Rice, S. D.; Collier, T. K.; Scholz, N. L.; Incardona, J. P. Sublethal exposure to crude oil during embryonic development alters cardiac morphology and reduces aerobic capacity in adult fish. *Proc. Natl. Acad. Sci. U. S. A.* **2011**, *108* (17), 7086−7090.

(5) Incardona, J. P.; Collier, T. K.; Scholz, N. L. Oil spills and fish health: Exposing the heart of the matter. *J. Exposure Sci. Environ. Epidemiol.* **2011**, *21* (1), 3−4.

(6) Esbaugh, A. J.; Mager, E. M.; Stieglitz, J. D.; Hoenig, R.; Brown, T. L.; French, B. L.; Linbo, T. L.; Lay, C.; Forth, H.; Scholz, N. L.; Incardona, J. P. The effects of weathering and chemical dispersion on Deepwater Horizon crude oil toxicity to mahi-mahi (*Coryphaena hippurus*) early life stages. *Sci. Total Environ.* **2016**, *543*, 644−651.

(7) Carls, M. G.; Meador, J. P. A perspective on the toxicity of petrogenic PAHs to developing fish embryos related to environmental chemistry. *Hum. Ecol. Risk Assess.* **2009**, *15* (6), 1084−1098.

(8) Bornstein, J. M.; Adams, J.; Hollebone, B.; King, T.; Hodson, P. V.; Brown, R. S. Effects-driven chemical fractionation of heavy fuel oil to isolate compounds toxic to trout embryos. *Environ. Toxicol. Chem.* **2014**, *33* (4), 814−824.

(9) Incardona, J. P.; Swarts, T. L.; Edmunds, R. C.; Linbo, T. L.; Aquilina-Beck, A.; Sloan, C. A.; Gardner, L. D.; Block, B. A.; Scholz, N. L. Exxon Valdez to Deepwater Horizon: Comparable toxicity of both crude oils to fish early life stages. *Aquat. Toxicol.* **2013**, *142*, 303−316.

(10) Jung, J. H.; Hicken, C. E.; Boyd, D.; Anulacion, B. F.; Carls, M. G.; Shim, W. J.; Incardona, J. P. Geologically distinct crude oils cause a common cardiotoxicity syndrome in developing zebrafish. *Chemosphere* **2013**, *91* (8), 1146−1155.

(11) Mager, E. M.; Esbaugh, A. J.; Stieglitz, J. D.; Hoenig, R.; Bodinier, C.; Incardona, J. P.; Scholz, N. L.; Benetti, D. D.; Grosell, M. Acute embryonic or juvenile exposure to Deepwater Horizon crude oil impairs the swimming performance of mahi-mahi (*Coryphaena hippurus*). *Environ. Sci. Technol.* **2014**, *48* (12), 7053−7061.

(12) Stieglitz, J. D.; Mager, E. M.; Hoenig, R.; Benetti, D. D.; Grosell, M. Impacts of Deepwater Horizon crude oil exposure on adult mahi-mahi (*Coryphaena hippurus*) swim performance. *Environ. Toxicol. Chem.* **2016**, DOI: 10.1002/etc.3436.

(13) Incardona, J. P.; Collier, T. K.; Scholz, N. L. Defects in cardiac function precede morphological abnormalities in fish embryos exposed to polycyclic aromatic hydrocarbons. *Toxicol. Appl. Pharmacol.* **2004**, *196* (2), 191−205.

(14) Huang, L.; Wang, C.; Zhang, Y.; Wu, M.; Zuo, Z. Phenanthrene causes ocular developmental toxicity in zebrafish embryos and the possible mechanisms involved. *J. Hazard. Mater.* **2013**, *261*, 172−180.

(15) Edmunds, R. C.; Gill, J. A.; Baldwin, D. H.; Linbo, T. L.; French, B. L.; Brown, T. L.; Esbaugh, A. J.; Mager, E. M.; Stieglitz, J.; Hoenig, R.; Benetti, D. Corresponding morphological and molecular indicators of crude oil toxicity to the developing hearts of mahi mahi. *Sci. Rep.* **2015**, *5*, 17326.

(16) Stieglitz, J. D.; Benetti, D. D.; Hoenig, R. H.; Sardenberg, B.; Welch, A. W.; Miralao, S. Environmentally conditioned, year-round volitional spawning of cobia (*Rachycentron canadum*) in broodstock maturation systems. *Aquacult. Res.* **2012**, *43* (10), 1557−1566.

(17) Buchfink, B.; Xie, C.; Huson, D. H. Fast and sensitive protein alignment using DIAMOND. *Nat. Methods* **2015**, *12* (1), 59−60.

(18) Love, M. I.; Huber, W.; Anders, S. Moderated estimation of fold change and dispersion for RNA-seq data with DESeq2. *Genome Biol.* **2014**, *15* (12), 1−21.

(19) Paolini, P.; Pick, D.; Lapira, J.; Sannino, G.; Pasqualini, L.; Ludka, C.; Sprague, L. J.; Zhang, X.; Bartolotta, E. A.; Vazquez-Hidalgo, E.; Barba, D. T. Developmental and extracellular matrix-remodeling processes in rosiglitazone-exposed neonatal rat cardiomyocytes. *Pharmacogenomics* **2014**, *15* (6), 759−774.

(20) Draghici, S.; Khatri, P.; Tarca, A. L.; Amin, K.; Done, A.; Voichita, C.; Georgescu, C.; Romero, R. A systems biology approach for pathway level analysis. *Genome Res.* **2007**, *17* (10), 1537−1545.

(21) Chen, J.; Bardes, E. E.; Aronow, B. J.; Jegga, A. G. ToppGene Suite for gene list enrichment analysis and candidate gene prioritization. *Nucleic Acids Res.* **2009**, *37* (suppl 2), W305−W311.

(22) Metzger, J. M.; Westfall, M. V. Covalent and noncovalent modification of thin filament action: the essential role of troponin in cardiac muscle regulation. *Circ. Res.* **2004**, *94* (2), 146−158.

(23) Handley-Goldstone, H. M.; Grow, M. W.; Stegeman, J. J. Cardiovascular gene expression profiles of dioxin exposure in zebrafish embryos. *Toxicol. Sci.* **2005**, *85* (1), 683−693.

(24) Brette, F.; Machado, B.; Cros, C.; Incardona, J. P.; Scholz, N. L.; Block, B. A. Crude oil impairs cardiac excitation-contraction coupling in fish. *Science* **2014**, *343* (6172), 772−776.

(25) Alexeyenko, A.; Wassenberg, D. M.; Lobenhofer, E. K.; Yen, J.; Linney, E.; Sonnhammer, E. L. L.; Meyer, J. N. Dynamic zebrafish interactome reveals transcriptional mechanisms of dioxin toxicity. *PLoS One* **2010**, *5* (5), e10465.

(26) Goodale, B. C.; La Du, J.; Tilton, S. C.; Sullivan, C. M.; Bisson, W. H.; Waters, K. M.; Tanguay, R. L. Ligand-specific transcriptional mechanisms underlie aryl hydrocarbon receptor-mediated developmental toxicity of oxygenated PAHs. *Toxicol. Sci.* **2015**, *147*, p.kfv139.

(27) Hofmann, K. P.; Heck, M. Light-induced protein-protein interactions on the rod photoreceptor disc membrane. In Lee AG. *Rhodopsin and G-Protein Linked Receptors, Part A*; JAI Press: Greenwich, CT. 1996; Vol 2 (2 Vol Set), pp 141−198.

(28) Freund, C. L.; Gregory-Evans, C. Y.; Furukawa, T.; Papaioannou, M.; Looser, J.; Ploder, L.; Bellingham, J.; Ng, D.; Herbrick, J. A. S.; Duncan, A.; Scherer, S. W. Cone-rod dystrophy due to mutations in a novel photoreceptor-specific homeobox gene (CRX) essential for maintenance of the photoreceptor. *Cell* **1997**, *91* (4), 543−53.

DOI: 10.1021/acs.est.6b02205
Environ. Sci. Technol. 2016, 50, 7842−7851

(29) Kawaguchi, M.; Sugahara, Y.; Watanabe, T.; Irie, K.; Ishida, M.; Kurokawa, D.; Kitamura, S. I.; Takata, H.; Handoh, I. C.; Nakayama, K.; Murakami, Y. Nervous system disruption and concomitant behavioral abnormality in early hatched pufferfish larvae exposed to heavy oil. *Environ. Sci. Pollut. Res.* **2012**, *19* (7), 2488−2497.
(30) Hood, D. B.; Sheng, L.; Ding, X. X.; Ferguson, M.; McCallister, M.; Rhoades, R.; Maguire, M.; Ramesh, A.; Aschner, M.; Campbell, D.; Levitt, P.; Hood, D. B. Prenatal polycyclic aromatic hydrocarbon exposure leads to behavioral deficits and downregulation of receptor tyrosine kinase, MET. *Toxicol. Sci.* **2010**, *118* (2), 625−634.
(31) Gao, D.; Wu, M.; Wang, C.; Wang, Y.; Zuo, Z. Chronic exposure to low benzo [a] pyrene level causes neurodegenerative disease-like syndromes in zebrafish (*Danio rerio*). *Aquat. Toxicol.* **2015**, *167*, 200−208.
(32) Tissingh, G.; Booij, J.; Bergmans, P.; Winogrodzka, A.; Janssen, A. G.; Van Royen, E. A.; Stoof, J. C.; Wolters, E. C. Iodine-123-N-(omega)-fluoropropyl-2(beta)-carbomethoxy-3 (beta)-(4-iodophenyl) tropae SPECT in healthy controlsand early-stage, drug-naive Parkinson's disease. *J. Nucl. Med.* **1998**, *39* (7), 1143−1148.
(33) Fink, C. C.; Meyer, T. Molecular mechanisms of CaMKII activation in neuronal plasticity. *Curr. Opin. Neurobiol.* **2002**, *12* (3), 293−299.
(34) Kazama, H.; Nose, A.; Morimoto-Tanifuji, T. Synaptic components necessary for retrograde signaling triggered by calcium/calmodulin-dependent protein kinase II during synaptogenesis. *Neuroscience* **2007**, *145* (3), 1007−1015.
(35) He, C.; Wang, C.; Zhou, Y.; Li, J.; Zuo, Z. Embryonic exposure to benzo (a) pyrene influences neural development and function in rockfish (*Sebastiscus marmoratus*). *NeuroToxicology* **2012**, *33* (4), 758−762.
(36) Stolboushkina, E. A.; Garber, M. B. Eukaryotic type translation initiation factor 2: Structure−functional aspects. *Biochemistry (Moscow)* **2011**, *76* (3), 283−294.
(37) Wek, R. C.; Jiang, H. Y.; Anthony, T. G. Coping with stress: eIF2 kinases and translational control. *Biochem. Soc. Trans.* **2006**, *34* (Pt 1), 7−11.
(38) Fang, X.; Corrales, J.; Thornton, C.; Clerk, T.; Scheffler, B. E.; Willett, K. L. Transcriptomic changes in zebrafish embryos and larvae following benzo [a] pyrene exposure. *Toxicol. Sci.* **2015**, *146* (2), 395−411.
(39) Wang, Q.; Jiang, H.; Fan, Y.; Huang, X.; Shen, J.; Qi, H.; Li, Q.; Lu, X.; Shao, J. Phosphorylation of the α-subunit of the eukaryotic initiation factor-2 (eIF2α) alleviates benzo [a] pyrene-7, 8-diol-9, 10-epoxide induced cell cycle arrest and apoptosis in human cells. *Environ. Toxicol. Pharmacol.* **2011**, *31* (1), 18−24.
(40) Irish, J. C.; Mills, J. N.; Turner-Ivey, B.; Wilson, R. C.; Guest, S. T.; Rutkovsky, A.; Dombkowski, A.; Kappler, C. S.; Hardiman, G.; Ethier, S. P. Amplification of WHSC1L1 regulates expression and estrogen-independent activation of ERα in SUM-44 breast cancer cells and is associated with ERα over-expression in breast cancer. *Mol. Oncol.* **2016**, *10* (6), 850−865.
(41) Hardiman, G.; Hazard, S. E.; Savage, S. J.; Wilson, R. C.; Smith, M. T.; Hollis, B. W.; Halbert, C. H.; Gattoni-Celli, S. Systems analysis of the prostate transcriptome in African American men compared to European American men. *Pharmacogenomics*, **2016** DOI: 10.2217/pgs-2016-0025

DOI: 10.1021/acs.est.6b02205
Environ. Sci. Technol. 2016, 50, 7842−7851